Supplementary Figures

The Nuclear Receptor LXRα controls the functional specialization of splenic macrophages

Noelia A-Gonzalez[1,2,3,11], Jose A. Guillen[1,2,11], Germán Gallardo[2,11], Mercedes Diaz[1,2,11], Juan V. de la Rosa[2], Irene H. Hernandez[1,2], Maria Casanova-Acebes[3], Felix Lopez[2], Carlos Tabraue[2], Susana Beceiro[1,2], Cynthia Hong[4], Pedro C. Lara[5], Miguel Andujar[6], Satoko Arai[7], Toru Miyazaki[7], Senlin Li[8,9], Angel L. Corbi[10], Peter Tontonoz[4], Andres Hidalgo[3] and Antonio Castrillo[1,2]

[1]Instituto de Investigaciones Biomédicas "Alberto Sols" CSIC-Universidad Autonóma de Madrid, Madrid Spain and [2]Unidad Asociada de Biomedicina IIBM CSIC-Universidad de Las Palmas de Gran Canaria, Las Palmas Spain.[3]Department of Epidemiology, Atherothrombosis and Imaging, Centro Nacional de Investigaciones Cardiovasculares, CNIC Madrid, Spain.[4]Howard Hughes Medical Institute, Department of Pathology and Laboratory Medicine, University of California Los Angeles, California USA.[5]Servicio de Oncología Radioterápica, Hospital Universitario de Gran Canaria Dr. Negrín, Las Palmas, Spain.[6]Servicio de Patología, Hospital Universitario Materno-Infantil de Las Palmas, Spain[7]Laboratory of Molecular Biomedicine for Pathogenesis, Center for Disease Biology and Integrative Medicine, Faculty of Medicine, University of Tokyo, Japan.[8]Departments of Medicine and Pharmacology, University of Texas Health Science Center, and [9]South Texas Veterans Health Care System, San Antonio, Texas, USA.[10]Centro de Investigaciones Biológicas, Consejo Superior de Investigaciones Científicas, Madrid, Spain.

[11]These authors contributed equally to this work

Correspondence should be addressed to A.C. (acastrillo@iib.uam.es)

Antonio Castrillo, Ph.D.

Instituto de Investigaciones Biomédicas "Alberto Sols"

Consejo Superior de Investigaciones Científicas-Universidad Autónoma de Madrid. Madrid, Spain and Unidad Asociada de Biomedicina Instituto de Investigaciones Biomédicas "Alberto Sols" IIBM CSIC-Universidad de Las Palmas de Gran Canaria, Spain

Email: acastrillo@iib.uam.es

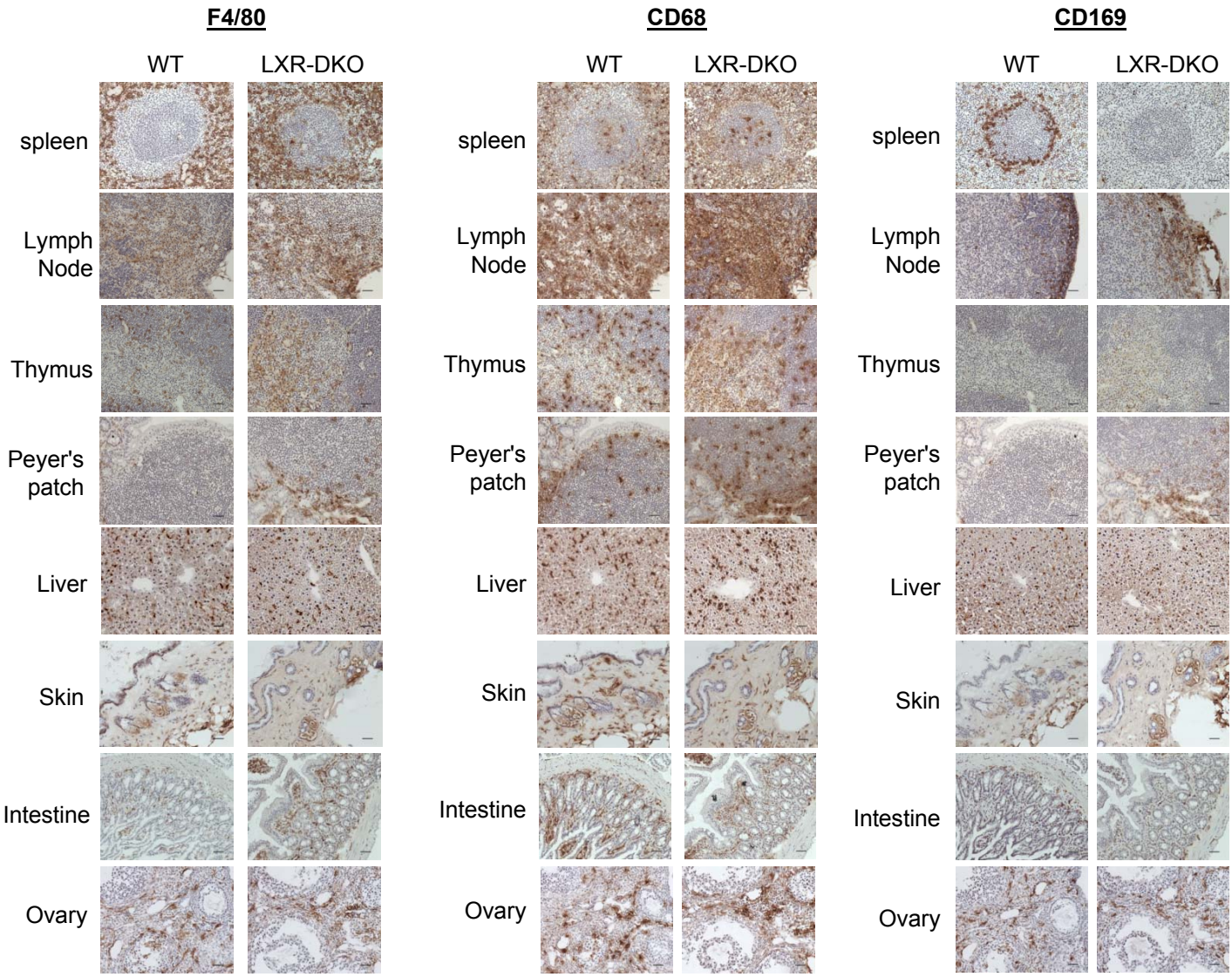

Supplementary Fig. 1: Distribution of tissue macrophage populations in WT and LXR deficient mice. Immunohistochemical localization of F4/80, CD68 and CD169 macrophages in several tissues obtained from 4-week old WT and LXR-DKO mice. Representative pictures from two independent experiments with n=4 mice per genotype are shown. Scale bar represents 50μm.

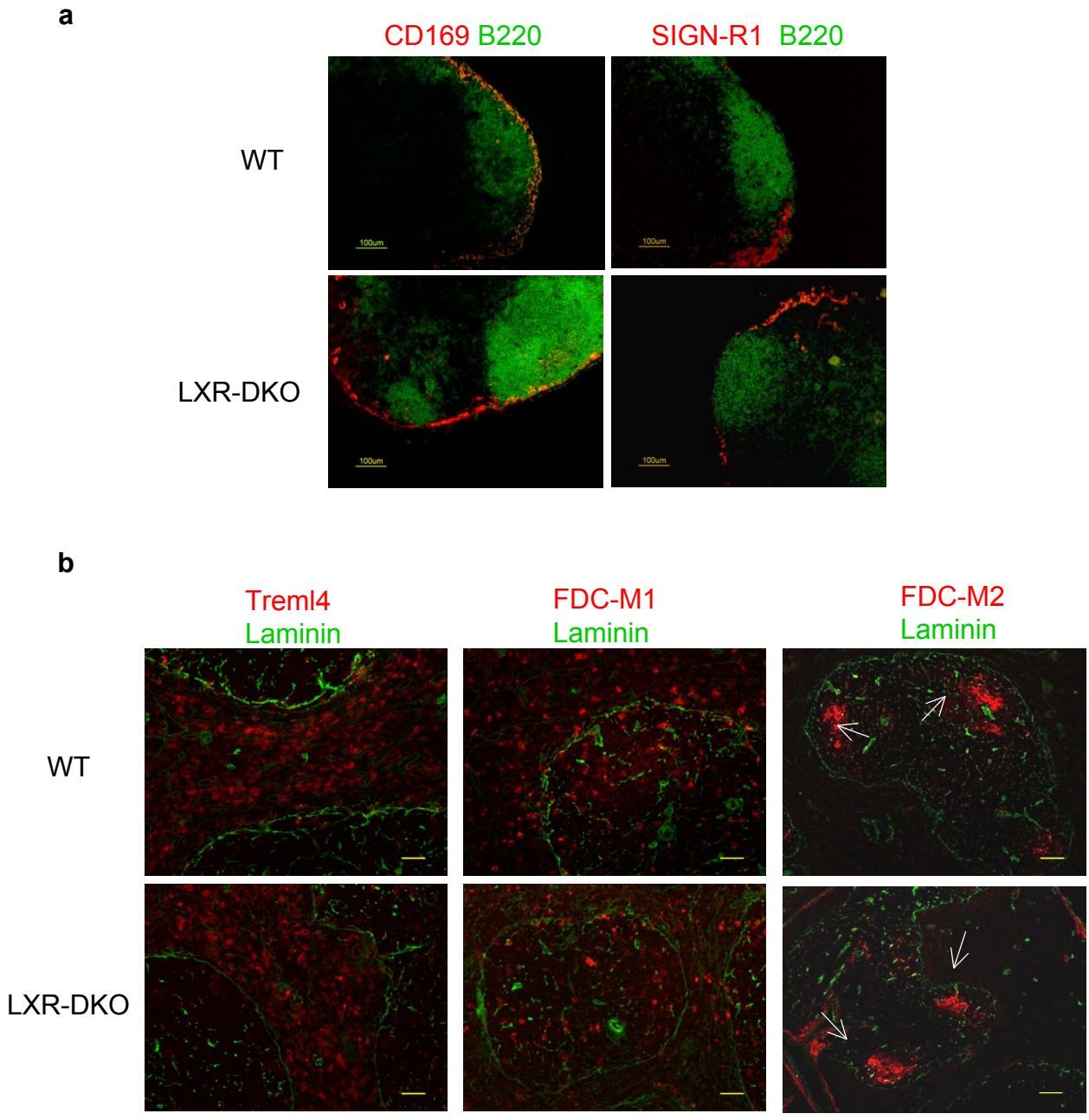

Supplementary Fig.2: LXR-DKO mice present normal distribution of additional myeloid cells in the spleen and lymph node. (a) Immunofluorescence analysis of lymph node sections from WT and LXR-DKO mice stained with CD169, SIGN-R1 and B220 antibodies. (b) Immunoflorescence analysis of spleen sections from WT and LXR-DKO mice stained with dendritic cell markers (TremL4+, FDC-M1+, and FDC-M2+ cells) relative to Laminin+ cells. Representative pictures from three (a) and two (b) independent experiments with n=4 mice per genotype are shown. Scale bar represents 50 μm

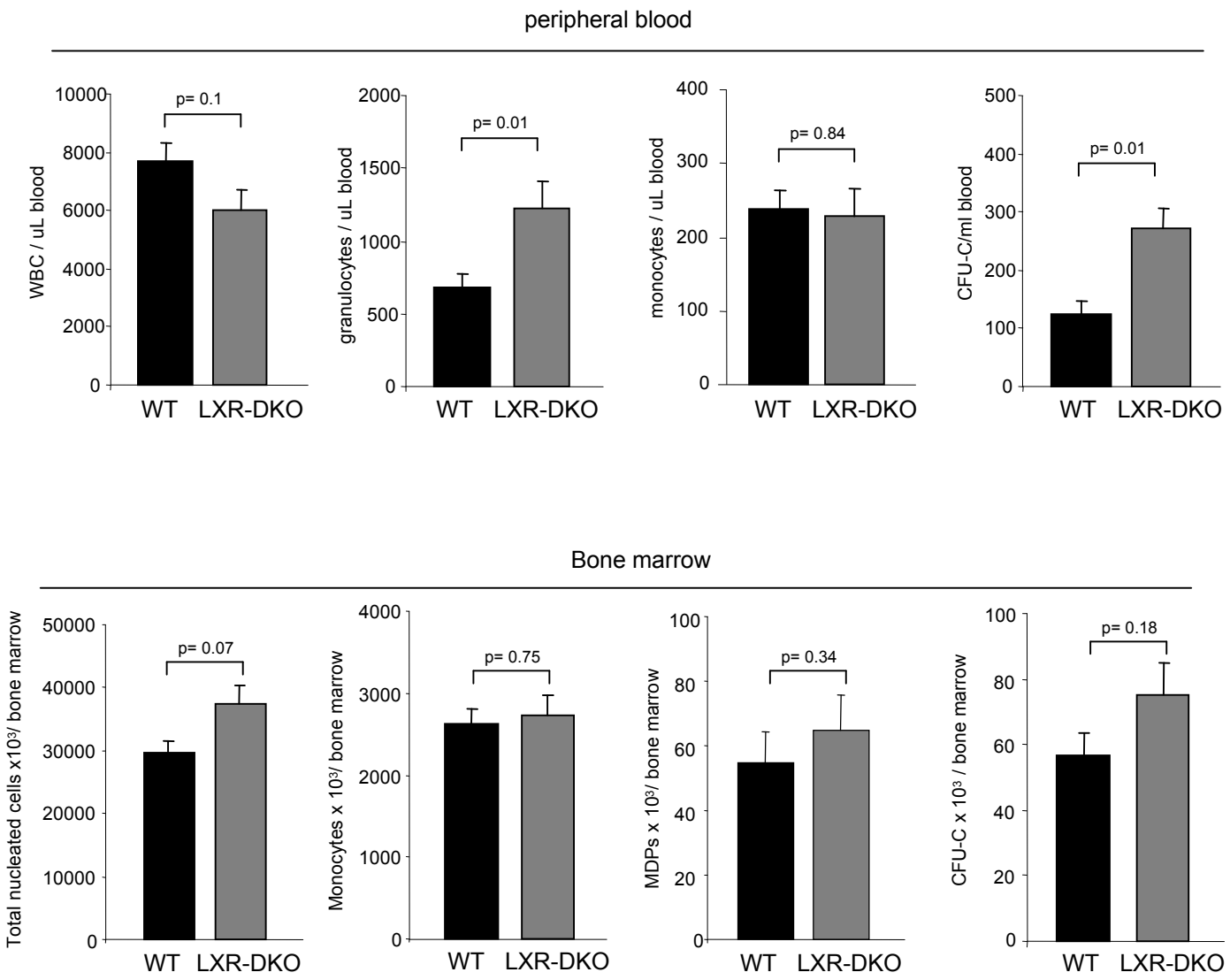

Supplementary Fig. 3: Frequency of bone marrow and peripheral blood monocytes and myeloid progenitors. BM cells from WT and LXR-DKO mice were collected and analized for CFU-C and MDPs (macrophage and DC precursor) progenitors (n=4). Blood was collected by retro-orbital injection from WT and DKO-mice (n=8) and blood counts quantified. Data represent mean +/- SEM from two independent experiments.

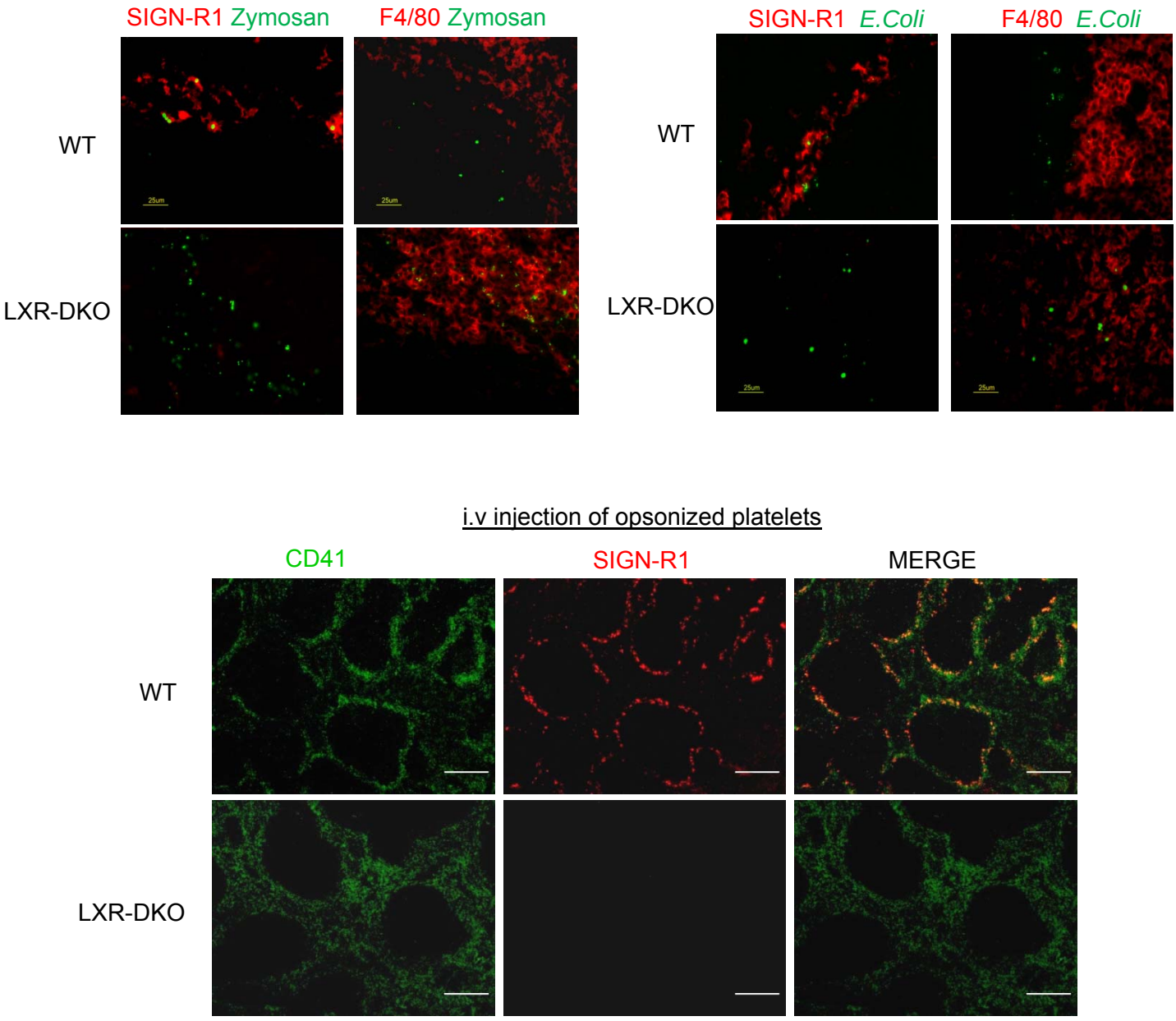

Supplementary Fig 4: Altered capture of blood-borne antigens by LXR-DKO spleen macrophages. Immunofluorescence analysis of spleen sections from WT and LXR-DKO mice stained with SIGN-R1 and F4/80 antibodies to detect MZ and RP macrophages and their association with zymosan and GFP-*E.coli* (top panels). Lower panel shows immunofluorescence analysis of spleen sections from WT and LXR-DKO mice injected with CD41-opsonized platelets, and stained with CD41 and SIGN-R1 antibodies; scale bar in this panel represents 300 μm. Pictures are representative of three independent experiments with n=5 mice per group.

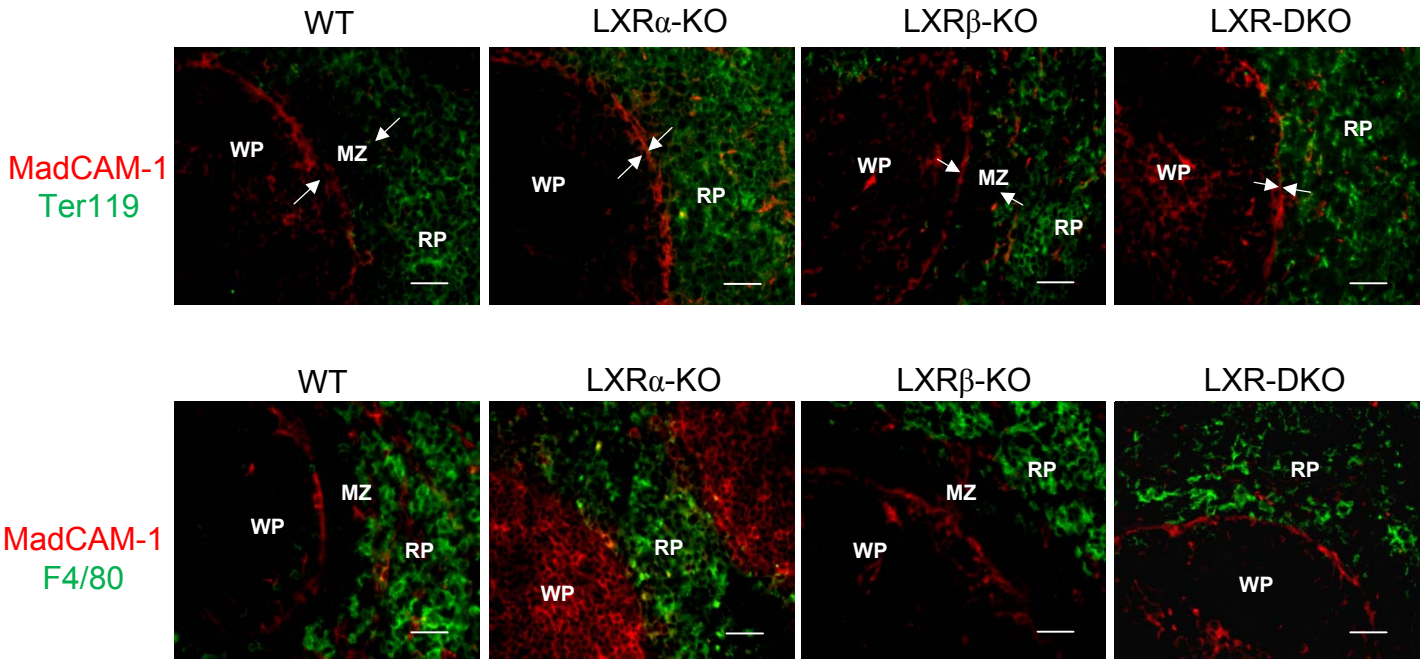

Supplementary Fig 5: Absence of marginal space in LXRα-KO and LXR-DKO mice. Immunofluorescence analysis of spleen sections from WT, LXRα-KO, LXRβ-KO, and LXR-DKO mice stained with MadCAM-1 (to detect marginal sinus lining cells) and Ter119 (RP erythrocytes, in a) or F4/80 (RP macrophages, in b). Representative pictures from three independent experiments with n = 3-4 mice per group are presented. Scale bar represents 50 μm

a

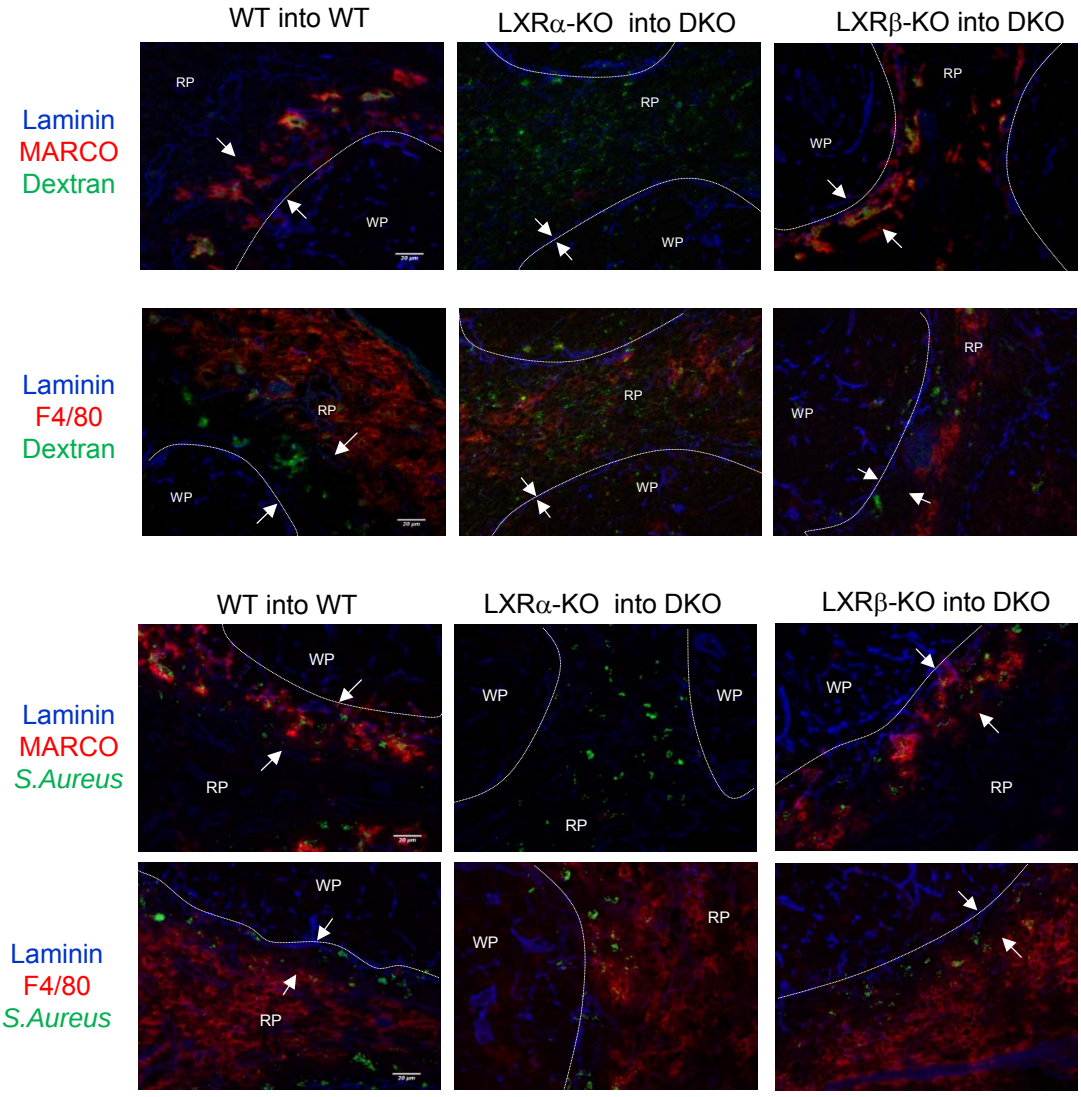

b

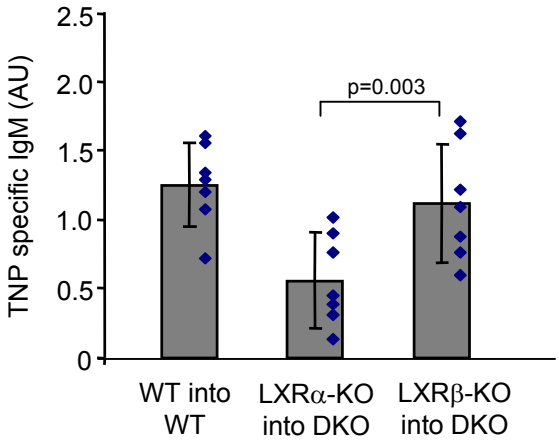

Supplementary Figure 6: LXRα activity in hematopoietic cells reconstitutes MZ functions in LXR-DKO mice. (a) WT and LXR-DKO mice were transplanted with the indicated BM donor progenitors and i.v. injected with dextran-FITC or AF488-*S.aureus* particles 12 weeks after transplantation. IF detection of MZ and RP macrophages in spleen sections obtained post injection. Dashed lines delimitate the border of the WP and the RP. Representative pictures from n=4 mice per group are presented. (b). Separate cohorts of WT and LXR-DKO mice were transplanted similar to (a). Mice were immunized with TNP-ficoll and serum samples were obtained 7 days after immunization. TNP-specific IgM titers were measured by ELISA. Each (◊) symbol represents individual mice (n=7).

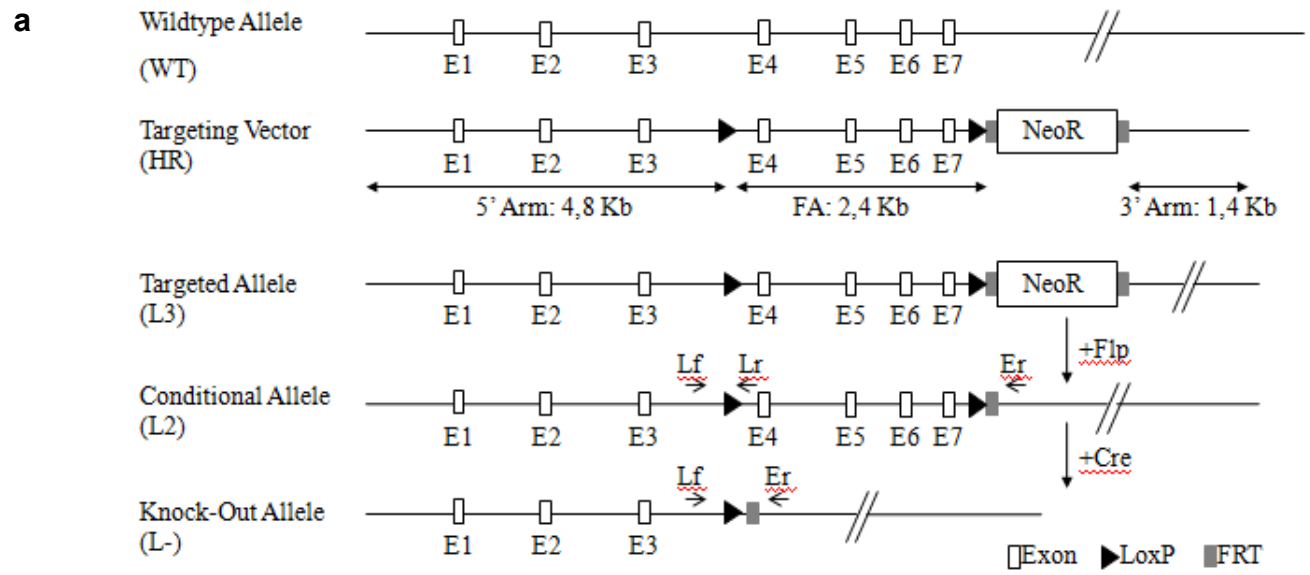

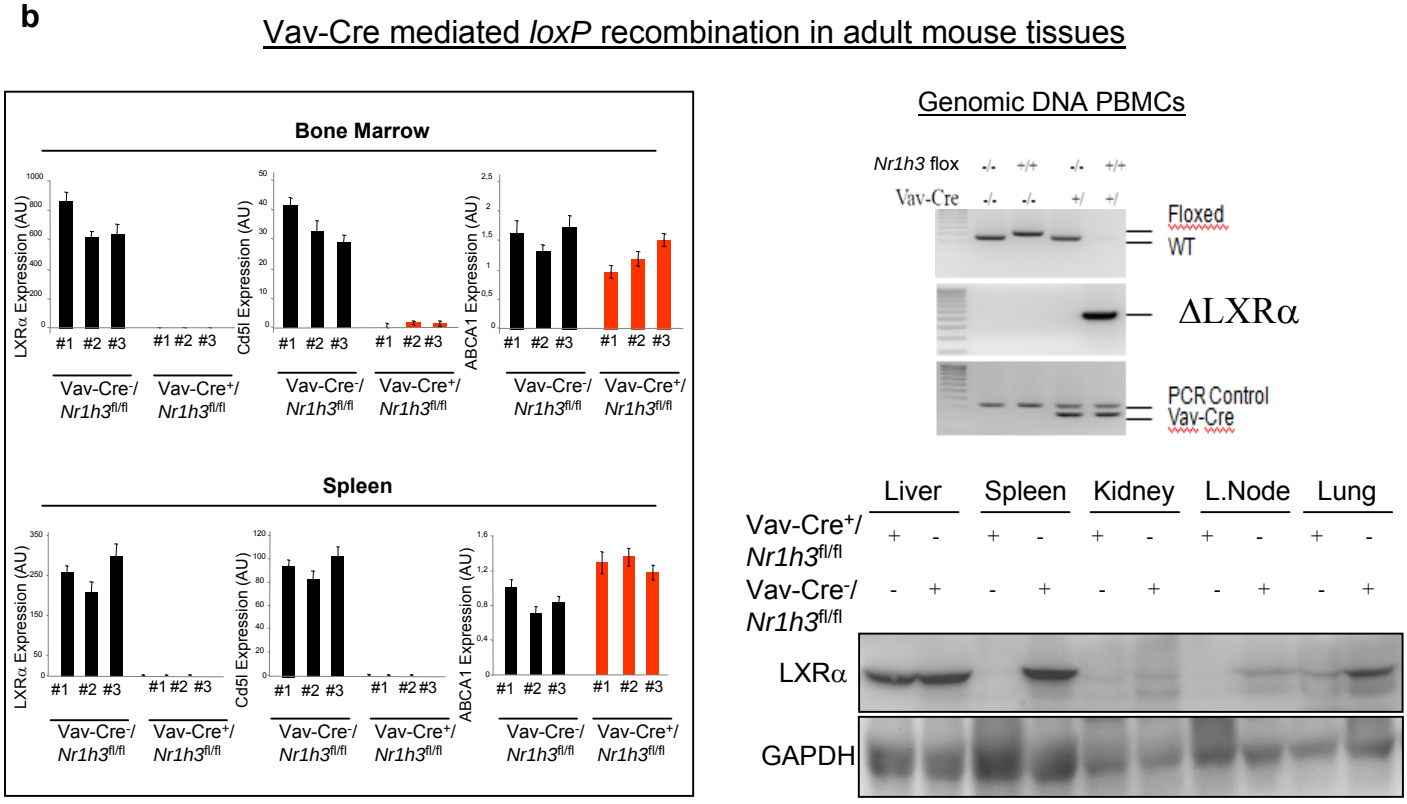

Supplementary Fig. 7: Generation of Vav-Cre^{+}*Nr1h3*$^{fl/fl}$ mice. (a) targeting strategy to disrupt LXRα expression in hematopoietic cells (b) PCR genotyping to identify *Nr1h3*$^{fl/fl}$ and Vav-Cre mice and immunoblot of LXRα and GADPH in liver, spleen, kidney, lymph node, and lung from Vav-Cre^{+} *Nr1h3*$^{fl/fl}$ and Vav-Cre^{-} *Nr1h3*$^{fl/fl}$ mice (right). Analysis of LXRα, Cd5l and ABCA1 transcript levels by real-time qPCR in individual Vav-Cre^{+} *Nr1h3*$^{fl/fl}$ and Vav-Cre^{-} *Nr1h3*$^{fl/fl}$ mice (left). Representative results from two independent experiments with n = 3-5 mice per group are presented

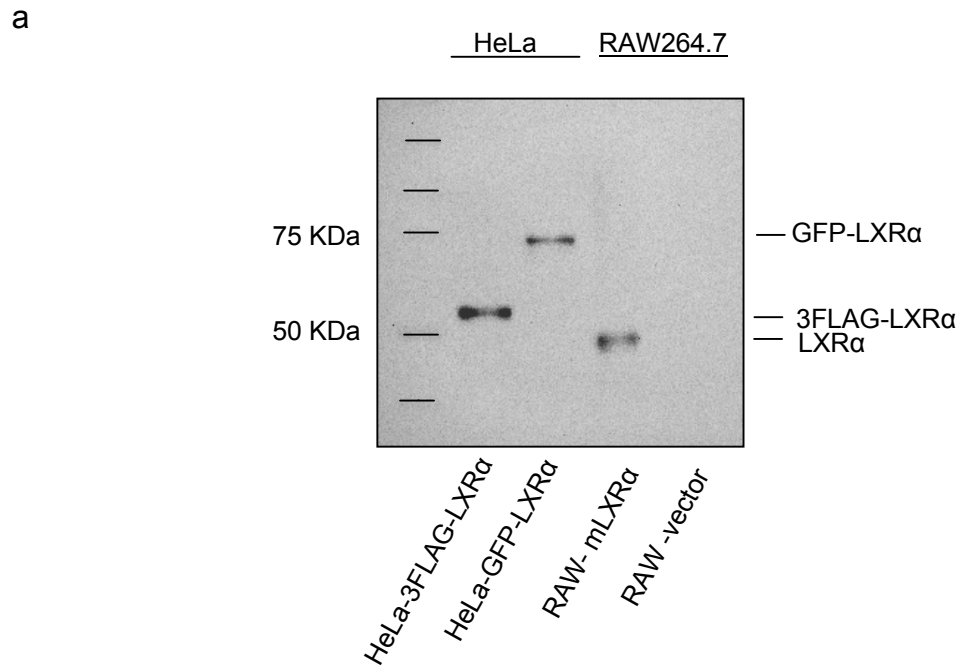

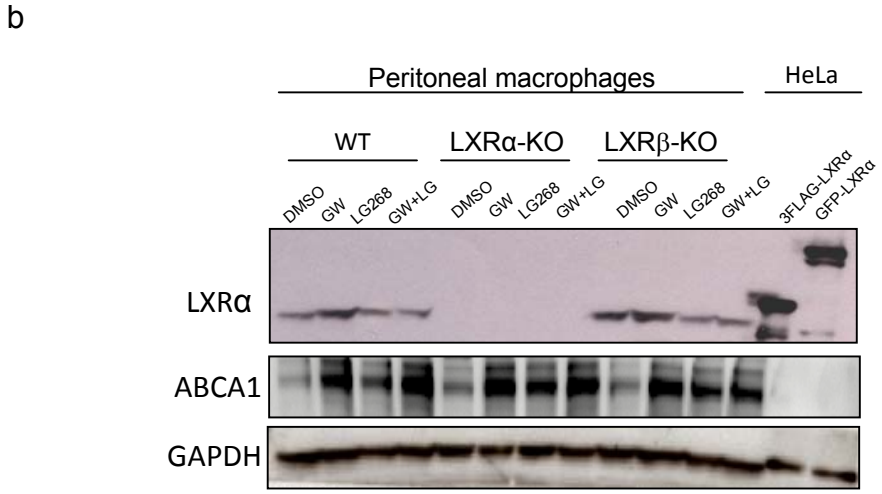

Supplementary Fig. 8: Validation of LXRα antibody. (a) Western blot analysis of LXRα in HeLa and RAW264.7 cells stably expressing LXRα, 3FLAG-LXRα or GFP-LXRα and vector control. (b) Western blot analysis of LXRα and ABCA1 expression in peritoneal macrophages from WT, LXRα-KO and LXRβ-KO treated with GW3965 (1 μM) and LG268 (0.1 μM) alone or in combination for 24 hours, and in HeLa cells expressing 3FLAG-LXRα or GFP-LXRα. GADPH protein expression was used as loading control.

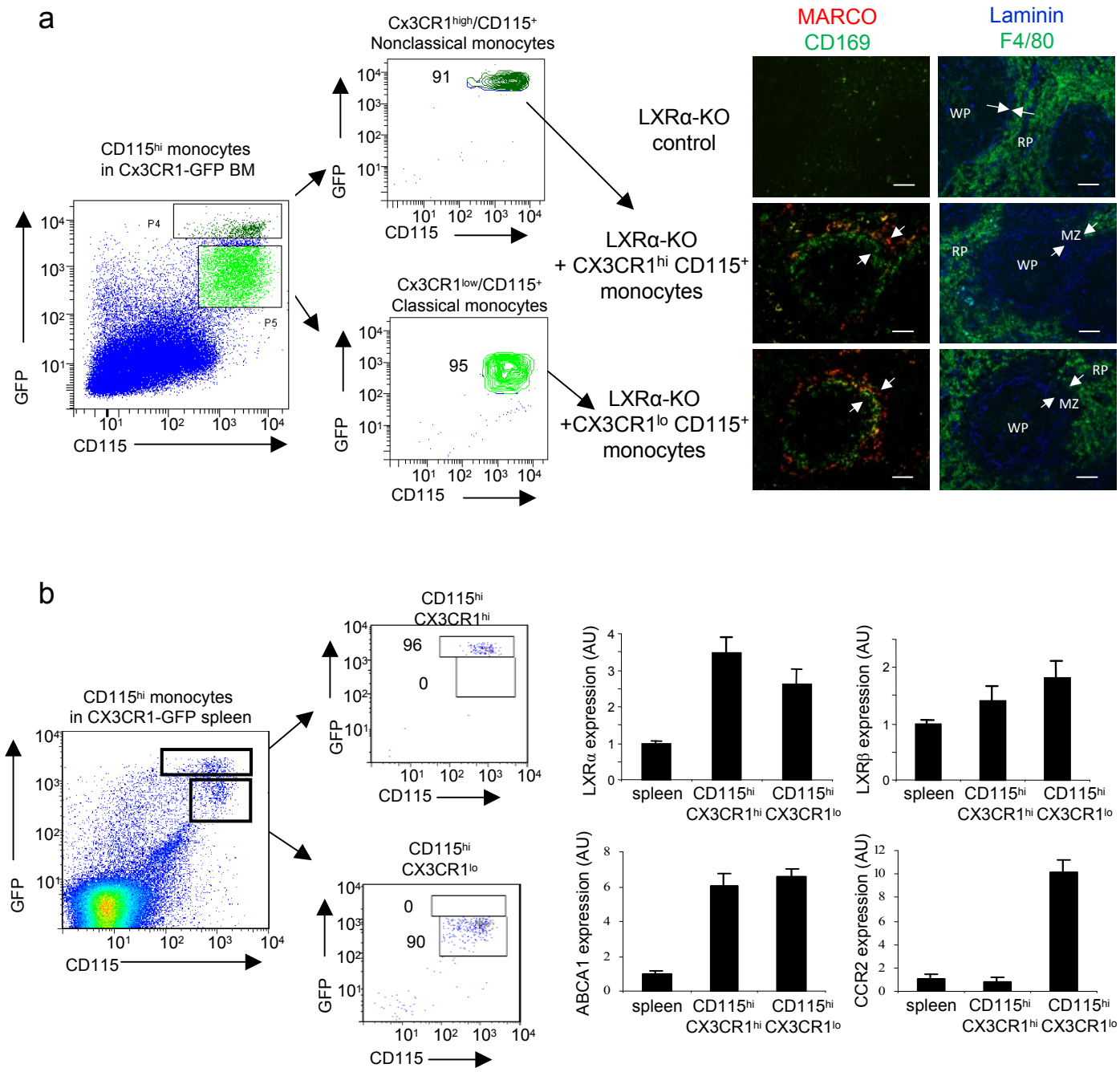

Supplementary Fig. 9: Reconstitution of MZ macrophages in LXRα-KO mice with classical or non-classical monocytes. (a) sorting strategy to separate CX3CR1^{lo}/CD115^{+} and CX3CR^{hi}/CD115^{+} monocytes from BM. Numbers within plots indicate the purity (%) of the sorted population. Right panel shows immunofluorescence analysis of spleen sections obtained from LXRα-KO mice after adoptive transfer of monocytes. Consecutive sections were stained with MARCO CD169 and Laminin F4/80. Representative pictures from two independent experiments with n=5 mice per group are presented. Scale bar represents 50 μm. (b) mRNA levels of LXRα, LXRβ, ABCA1 and CCR2 in spleen samples, and in purified monocytes (right panel). Bars indicate mean +/- SEM (n=3 mice). Data are representative of two independent experiments.

Abca1 FWD GCAGATCAAGCATCCCAACT
Abca1 REV CCAGAGAATGTT TCATTGTCCA

36b4 FWD ACTGGTCTAGGACCCGAGAAG
36b4 REV TCCCACCTTGTCTCCAGTCT

Marco FWD: GGCACCAAGGGAGACAAA
Marco REV: TCCCTTCATGCCCATGTC

Cd169 FWD: CTTGGGTCAGCCAACAGTTC
Cd169 REV: GGTGATGGTGAAACCTGGAC

Emr1 (F4/80) FWD: CTTTGGCTATGGGCTTCCAGTC
Emr1 (F4/80) REV: GCAAGGACAGAGTTTATCGTG

Cd5l FWD: TAGAGTAGTAAAAGCCAGAGGCC
Cd5l REV: AGCATTGAAGAACACCTCATCTAGG

Cd68 FWD: CAAGGTCCAGGGAGGTTGTG
Cd68 REV: CGGTACCCATCCCCACCTGTCTCTCTC

Nr1h3 FWD: CAACAGTGTAACAGGCGCT
Nr1h3 REV: TGCAATGGGCCAAGGC

Nr1h2 FWD: CCCCACAAGTTCTCTGGACACT
Nr1h2 REV: TGACGTGGCGGAGGTACTG

Ccr2 FWD: TTTGTTTTTGCAGATGATTCAA
Ccr2 REV: TGCCATCATAAAGGAGCCAT

Tim4 FWD: GGCTCCTTCTCACAAGAAACCACA
Tim4 REV: TCAGCTGTGAAGTGGATGGGAGA

Cd209b (SIGN-R1) FWD: CTGAAAACTGAACTCTTGTCCAGG
Cd209b (SIGN-R1) REV: CTGCTGCAGGAAGGTCTGCTC

Primers for the genotyping of *Nr1h3*$^{f/f}$ mice
Er: ATGCCTGAAAAGGGCATCAGATGCC
Lf: GGATTTGGAGAAGGTAAAGTCTCCC
Lr: TGGACTCAAGTGATCTTGTCTCAGC

Primers for the genotyping of Vav-Cre mice (obtained from JAX strain 008610 protocol)
Internal Positive Control FWD: CTAGGCCACAGAATTGAAAGATCT
Internal Positive Control REV: GTAGGTGGAAATTCTAGCATCATCC
Transgene FWD: AGATGCCAGGACATCAGGAACCTG
Transgene REV: ATCAGCCACACCAGACACAGAGATC

Supplementary Table 1: List of primers used in this study. Abreviations: FWD, forward primer; REV: reverse primer